

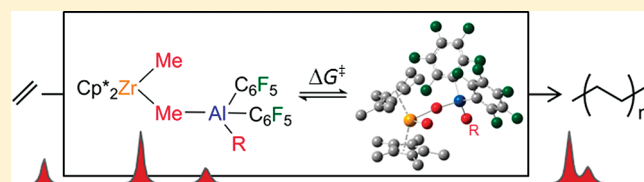
Structure, Dynamics, and Polymerization Activity of Zirconocenium Ion Pairs Generated with Boron-C₆F₅ Compounds and Al₂R₆

Déborah Mathis, Erik P. A. Couzijn, and Peter Chen*

Laboratorium für Organische Chemie, ETH Zürich, Wolfgang-Pauli-Strasse 10, CH-8093 Zürich, Switzerland

Supporting Information

ABSTRACT: The activation reaction of the olefin polymerization precatalyst Cp*₂ZrMe₂ with a boron-C₆F₅ compound (B(C₆F₅)₃, [Ph₃C][B(C₆F₅)₄]) and an aluminum alkyl species (Al₂Me₆, Al₂^tBu₆) is studied by NMR spectroscopy in order to determine the nature of the ion pairs that are formed preferentially. We show that a mixture of ion pairs with general formula Cp*₂Zr(Me)-μ-Me-E(C₆F₅)_{3-x}R_x (E = Al, B; x = 0, 1; R = Me, ^tBu) (1, 2a/b, 4) is generated due to a rapid transfer of pentafluorophenyl groups from boron to aluminum. Therefore, the molecular ratio of the activators determines the final composition of the ion pairs present in solution. When the pentafluorophenyl group transfer is suppressed, the ion pair Cp*₂Zr-(μ-Me)₂-AlMe₂ (5) forms irrespective of the reagent ratio. The high dynamics of these solutions is demonstrated by DNMR studies. Gibbs free energies of activation were determined of 13.6(12) kcal mol⁻¹ at 298 K for the cocatalyst exchange of ion pair Cp*₂Zr(Me)-μ-Me-Al(C₆F₅)₂Me (2a) and 13(2) kcal mol⁻¹ at 298 K for the methyl exchange in Al₂(C₆F₅)_xMe_{6-x} (x = 0, 1). Due to the stability of the ion pairs generated from the Cp*₂ZrMe₂ precatalyst at temperatures relevant for polymerization, correlations between activities in ethylene polymerization and the nature of the ion pairs can be established. All solutions containing the various ion pairs were found to be catalytically active in ethylene polymerization except that containing the ion pair 2a, which was attributed to the reduced Lewis acidity of the abstractor, as supported by DFT calculations.



INTRODUCTION

Despite the intensive research relating to the activation of zirconocene precatalysts for olefin polymerization,^{1–5} the nature and molecular ratios of the various ion pairs present in solution often remain ill-defined when performing a polymerization. Yet, it is these ion pairs that are responsible for the formation of the active species. The difficulty in predicting the outcome of a polymerization is mainly due to the lability of the catalytic system and its high sensitivity to any variation in reaction conditions. Even minimal changes in polymerization conditions can have a substantial influence on the catalytic activity and on the molecular structure of the formed polymer.⁶ Thus, it is essential to identify the nature of the ion pairs, the conditions under which they are generated, and their catalytic activities in olefin polymerization.

A good activator for metallocene precatalysts should both generate the cationic active species [L₂MR]⁺ and provide a weakly coordinating counteranion. The counteranion should stabilize the highly electrophilic 14-electron active species but should also be easily displaceable to allow olefin coordination.² The geometry and thermodynamic nature of the cation–anion interaction is of central importance for the catalytic activity, as reported by Marks and co-workers.^{7,8} Methylaluminoxane (MAO) is still the most commonly used activator in industry because it both generates large, weakly coordinating counteranions and has good scavenging properties.⁹ However, the mechanism of activation is better studied using reagents with a

well-defined structure, such as boron-C₆F₅ compounds (e.g., tris(pentafluorophenyl)borane (B(C₆F₅)₃) or tetrakis(pentafluorophenyl)borate ([Ph₃C][B(C₆F₅)₄])).² The activation of metallocenes with exclusively a boron-C₆F₅ compound is the subject of many reports,^{8,10–13} but it is well established that the use of an aluminum alkyl species as co-activator significantly improves the activity and stability of the catalytic system.¹⁴ One role of the aluminum alkyl species is to scavenge impurities, yet it may also be involved in the formation of the ion pairs.³

In this work, we investigate the reaction of boron-C₆F₅ compounds (B(C₆F₅)₃, [Ph₃C][B(C₆F₅)₄]) and Al₂R₆ (R = Me, ^tBu)¹⁵ with Cp*₂ZrMe₂ (Cp* = pentamethylcyclopentadienyl) by ¹H and ¹⁹F nuclear magnetic resonance (NMR) spectroscopy. We show that the combination of activators and their molecular ratios determine the final composition of the catalyst solution, which in general contains several ion pairs rather than a single one. Kinetic parameters for the structural rearrangement of the ion pairs are determined by variable-temperature dynamic NMR experiments. Furthermore, density functional theory (DFT) calculations are presented for obtaining geometrical parameters of the ion pairs. Lastly, the solutions containing the various ion pairs are tested for their catalytic activity in ethylene polymerization. The Cp*₂ZrMe₂ precatalyst presents the advantage that the ion pairs generated by reaction with the activators are stable

Received: May 4, 2011

Published: June 27, 2011

under conditions close to those for ethylene polymerization, providing a system uniquely well suited for studying the activation mechanism. Thus, correlations between the structural parameters of the different ion pairs, the strength of the Lewis acid activator, and the polymerization activities are discussed.

EXPERIMENTAL SECTION

All air- and/or water-sensitive compounds were handled under an inert atmosphere using standard Schlenk and glovebox techniques. Ethylene (N35 grade, > 99.95%, PanGas), bis(pentamethylcyclopentadienyl)zirconium dichloride ($\text{Cp}^*_2\text{ZrCl}_2$, 97%, Acros), tris(pentafluorophenyl)boron ($\text{B}(\text{C}_6\text{F}_5)_3$, min. 97%, Strem), trityl tetrakis(pentafluorophenyl)borate ($[\text{Ph}_3\text{C}][\text{B}(\text{C}_6\text{F}_5)_4]$, 97%, Acros), trimethylaluminum solution (TMA, 2.0 M in toluene, Aldrich), triisobutylaluminum solution (TIBA, 1.1 M in toluene, Acros), and methyl lithium solution (1.6 M in diethyl ether, Acros) were obtained commercially and used without further purification. Research-grade solvents were distilled from sodium (hexane, toluene) or Na/K alloy (diethyl ether) under nitrogen. Toluene- d_8 was stirred with Na/K alloy for 24 h and vacuum transferred. Solutions of trimethylaluminum (0.95 M) and triisobutylaluminum in toluene- d_8 (0.52 M) were prepared from pure trimethylaluminum (min. 98%, ABCR) and pure triisobutylaluminum (Aldrich). Bis(pentamethylcyclopentadienyl)zirconium dimethyl ($\text{Cp}^*_2\text{ZrMe}_2$) was synthesized according to a literature procedure.²³

NMR spectra were recorded on Varian Gemini 300 and Bruker ARX 300 instruments (^1H , 300 MHz; ^{19}F , 282 MHz). ^1H chemical shifts are reported in ppm relative to tetramethylsilane, using residual solvent protons as internal standard (toluene- d_7 : ^1H : 2.03 ppm (quintuplet)). ^{19}F chemical shifts are referenced externally to CF_3Cl .

DFT calculations were performed using the Gaussian 09 package. The M06-L²⁴ density functional was used with the SDD basis set and an automatic density-fitting basis for full optimization of the geometries. A frequency calculation was performed for each stationary point to confirm that it is a minimum.

NMR Experiments. For a typical NMR experiment, solutions of $\text{Cp}^*_2\text{ZrMe}_2$ precatalyst (7.5×10^{-2} M), of $\text{B}(\text{C}_6\text{F}_5)_3$ or $[\text{Ph}_3\text{C}][\text{B}(\text{C}_6\text{F}_5)_4]$ activator, and of Al_2Me_6 or Al_2^iBu_6 co-activator (7.5×10^{-2} M \times equiv((co)activator vs Zr)) in toluene- d_8 were prepared in a glovebox. The activators (0.2 mL of each solution) were mixed in a J. Young NMR tube for 10 min, after which the precatalyst solution (0.2 mL) was added, affording a final Zr concentration of 2.5×10^{-2} M in 0.6 mL of toluene- d_8 .

For variable-temperature dynamic NMR (over the range -80 to 80 °C at every 20 °C), the NMR probe was equilibrated for 10 min at the desired temperature before data acquisition. The spectra were analyzed with the program iNMR,²⁵ the internal line broadening at each temperature was determined from the ^1H signal of the Cp^* ligands, and the line shapes were simulated to afford experimental exchange rate constants k . The thermodynamic parameters ΔH^\ddagger , ΔS^\ddagger , and ΔG^\ddagger and their standard deviations were determined from linear regression analysis of Eyring plots of $\ln(k/T)$ vs $1/T$.

Polymerization Experiments. Toluene solutions of precatalyst $\text{Cp}^*_2\text{ZrMe}_2$ (7×10^{-3} M, 5 mL), of $\text{B}(\text{C}_6\text{F}_5)_3$ or $[\text{Ph}_3\text{C}][\text{B}(\text{C}_6\text{F}_5)_4]$ (1.4×10^{-2} M, 10 mL), and of Al_2Me_6 (3.5×10^{-2} M, 5 mL) or Al_2^iBu_6 (7×10^{-2} M, 5 mL) were prepared under an argon atmosphere and used for a series of five polymerization experiments. For each experiment, the required equivalents of each activator relative to 7×10^{-2} mmol Zr were combined in a 50 mL glass reactor, and toluene was added to attain a total volume of 5.5 mL. The mixture was aged for 10 min at 40 °C, after which the precatalyst solution (1 mL) was added and the reaction mixed for 3 min. After preactivation, the reaction was pressurized with ethylene to a controlled total pressure of 2 bar (1 bar Ar and 1 bar ethylene) and quenched after 3 min with HCl/MeOH solution.

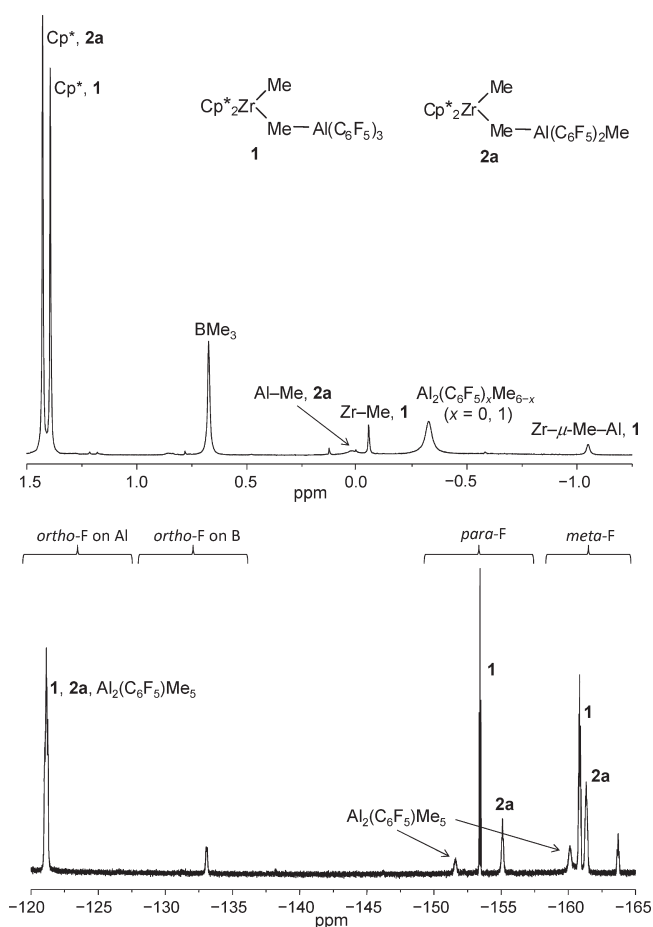


Figure 1. ^1H (top) and ^{19}F (bottom) NMR spectra in toluene- d_8 at 20 °C of the reaction between $\text{B}(\text{C}_6\text{F}_5)_3$, Al_2Me_6 , and $\text{Cp}^*_2\text{ZrMe}_2$ (ratio 1:2:1) and with residual solvent protons as internal standard (toluene- d_7 : ^1H : 2.03 ppm (quintuplet)). ^{19}F chemical shifts are referenced externally to CF_3Cl .

The polymers were filtered, vacuum-dried overnight, and weighed. Polymerization activities were derived from the amount of dried material produced in milligrams per mole of precatalyst per ethylene pressure in bar per hour.

GPC. The molecular weight distributions of the produced polymers were determined by gel permeation chromatography (PL-GPC 220) at 150 °C using 1,2,4-trichlorobenzene as solvent at a flow rate of 1.0 mL min^{-1} and with refractive index and viscosimetry detection. Two different sets of columns were used ($2 \times$ PLgel 5 μm MIXED-D and $2 \times$ PLgel 10 μm MIXED-B), and the instrument was calibrated using 1 mg mL^{-1} solutions of monodisperse fractions of atactic polystyrene standards (Fluka) with a universal calibration. Polyethylene samples with known molecular masses and polydispersities were measured as reference.

RESULTS AND DISCUSSION

I. Characterization of the Zirconocenium Ion Pairs by ^1H and ^{19}F NMR Spectroscopy. *a. Activation of $\text{Cp}^*_2\text{ZrMe}_2$ with $\text{B}(\text{C}_6\text{F}_5)_3$ and Al_2R_6 .* ^1H and ^{19}F NMR spectroscopy was used to determine the outcome of the reaction of $\text{B}(\text{C}_6\text{F}_5)_3$ with Al_2R_6 ($\text{R} = \text{Me}, ^i\text{Bu}$)¹⁵ and $\text{Cp}^*_2\text{ZrMe}_2$. In a typical experiment, $\text{B}(\text{C}_6\text{F}_5)_3$ and Al_2R_6 were mixed in toluene- d_8 for 10 min, after which a solution of $\text{Cp}^*_2\text{ZrMe}_2$ was added. The experiment was performed with several reactant molecular ratios, and ^1H and ^{19}F NMR spectra were recorded. Typical spectra are shown in Figures 1 and 2 (see below for further explanation).

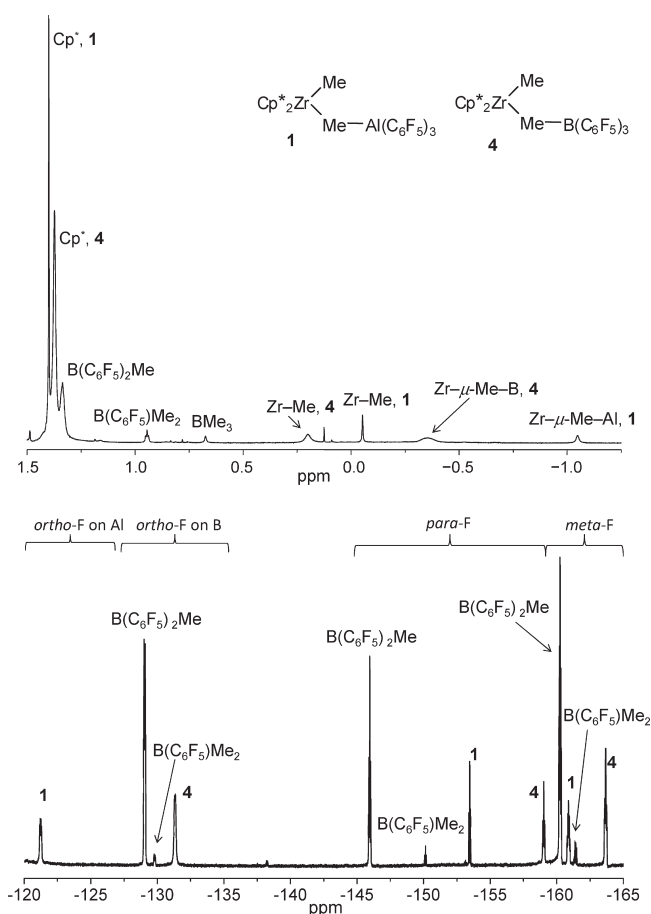
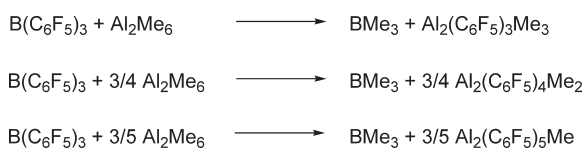


Figure 2. ^1H (top) and ^{19}F (bottom) NMR spectra in toluene- d_8 at 20 °C of the reaction between $\text{B}(\text{C}_6\text{F}_5)_3$, Al_2Me_6 , and $\text{Cp}^*_2\text{ZrMe}_2$ (ratio 2:1:1), resulting in a mixture of species **1**, **4**, and $\text{B}(\text{C}_6\text{F}_5)_x\text{Me}_{3-x}$.

Scheme 1. Exchange of Aryl and Alkyl Groups between B and Al Centers^a



^a The composition of the ligands on Al depends on the initial ratio of the reagents.¹⁸

Boron- C_6F_5 compounds may undergo rapid exchange of the pentafluorophenyl ligands for alkyl groups of Al_2R_6 .^{16–22} This reaction is often classified as a deactivation pathway¹⁶ and is fast in apolar solvents such as toluene but almost totally suppressed in coordinating solvents such as THF and ether.¹⁸ The driving force for the transmetalation is the formation of $\text{Al}-\text{C}_6\text{F}_5$ bonds, which are stronger compared to $\text{Al}-\text{alkyl}$ bonds than the corresponding $\text{B}-\text{C}_6\text{F}_5$ vs $\text{B}-\text{alkyl}$ bonds,¹⁹ leading to the transfer of all pentafluorophenyl groups to aluminum. Although the metallocene is not required for the reaction to occur, we cannot exclude that its presence might influence the reaction rate.²⁰ The final composition of a mixture of boron- C_6F_5 compounds and Al_2R_6 is dependent on the initial ratio of the reactants, as depicted in Scheme 1. The ratio between $\text{B}(\text{C}_6\text{F}_5)_3$ and Al_2R_6 therefore primarily determines which ion pairs are

Scheme 2. The Formation of Various Ion Pairs Depends on the Ratio between $\text{B}(\text{C}_6\text{F}_5)_3$ and Al_2R_6 ($\text{R} = \text{Me}, ^i\text{Bu}$) in the Reaction with $\text{Cp}^*_2\text{ZrMe}_2$

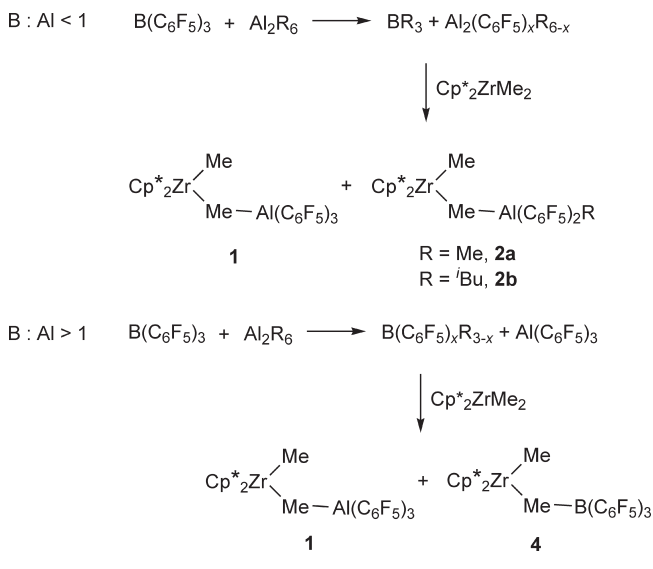


Table 1. Relative Amounts of the Ion Pairs **1** and **2a** Generated in Solution by Reaction of $\text{B}(\text{C}_6\text{F}_5)_3$, Al_2Me_6 , and $\text{Cp}^*_2\text{ZrMe}_2$ at Different Molecular Ratios^a

B:Al:Zr	1 (%)	2a (%)
1:1:1	66	34
1:2:1	51	49
1:5:1	25	75
1:10:1	14	86

^a The percentages of ion pairs **1** and **2a** were determined by integration of the corresponding Cp^* signals in the ^1H NMR spectra (Figure S1).

formed when $\text{B}(\text{C}_6\text{F}_5)_3$, Al_2R_6 , and $\text{Cp}^*_2\text{ZrMe}_2$ are combined (Scheme 2).

With an excess of Al_2R_6 vs $\text{B}(\text{C}_6\text{F}_5)_3$ (ratio B:Al < 1, Scheme 2, top), all pentafluorophenyl ligands initially bound to boron are transferred to aluminum, affording a mixture of $\text{Al}_2(\text{C}_6\text{F}_5)_x\text{R}_{6-x}$ ($x = 0-6$) and BR_3 . The subsequent reaction with $\text{Cp}^*_2\text{ZrMe}_2$ results in a mixture of two methyl-bridged species, namely, the ion pairs $\text{Cp}^*_2\text{Zr}(\text{Me})-\mu\text{-Me}-\text{Al}(\text{C}_6\text{F}_5)_3$ (**1**) and $\text{Cp}^*_2\text{Zr}(\text{Me})-\mu\text{-Me}-\text{Al}(\text{C}_6\text{F}_5)_2\text{R}$ (**2a**, $\text{R} = \text{Me}$; **2b**, $\text{R} = ^i\text{Bu}$). Figure 1 depicts the ^1H and ^{19}F NMR spectra at 20 °C of the reaction of $\text{B}(\text{C}_6\text{F}_5)_3$ with Al_2Me_6 and $\text{Cp}^*_2\text{ZrMe}_2$ at a B:Al:Zr ratio of 1:2:1 in toluene- d_8 , showing the presence of ion pairs **1** and **2a** as well as residual $\text{Al}_2(\text{C}_6\text{F}_5)_x\text{Me}_{6-x}$ and BMe_3 . The ^1H NMR signals for the bridging and the Zr-terminal methyl groups of **2a** shift and broaden with increasing measurement temperature, indicating that ion pair **2a** can undergo relatively facile dissociation/recombination via neutral fragments (see below). At 20 °C, the exchange reaction is fast so that, under the spectroscopic conditions used, the signals coalesce and thus are not visible in the NMR spectrum. The molecular ratio of ion pairs **1** and **2a** correlates with the initial ratio of the reagents (Table 1 and Figure S1). Figure S1 shows the stacked ^1H NMR spectra for four reagent molecular ratios (B:Al:Zr = 1:1:1; 1:2:1; 1:5:1, and 1:10:1) at 20 and -80 °C. With increasing amount of Al_2Me_6

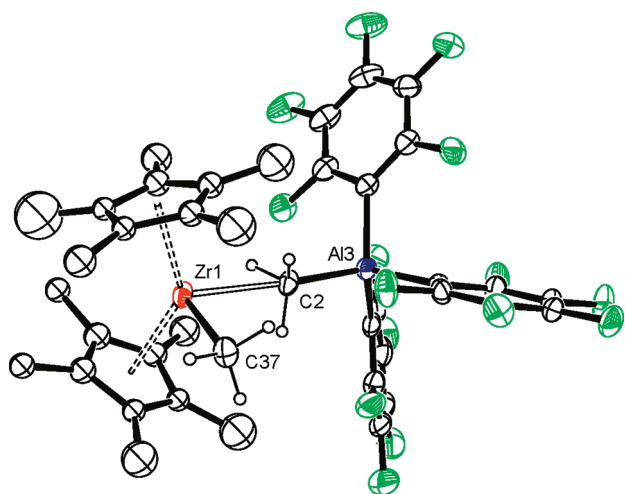


Figure 3. ORTEP representation of the X-ray crystal structure of ion pair 1. Ellipsoids are drawn at 30% probability. The crystal structure is disordered with respect to the Cp* orientation; the major of the two refined positions is shown (occupation 56%). The hydrogen atoms on the Cp* ligands are omitted for clarity. Selected distances [Å] and angles [deg]: Zr1–C37 2.246(7), Zr1–C2 2.550(6), C2–Al3 2.008(6), C37–Zr1–C2 90.6(2), Zr1–C2–Al3 176.5(3).

vs Cp*₂ZrMe₂, the intensity of the Cp* signal of ion pair 2a (δ 1.45) markedly increases at the expense of that of ion pair 1 (δ 1.40).

Using Al₂^{*i*}Bu₆ as co-activator, a mixture was obtained containing ion pairs 1 and Cp*₂Zr(Me)– μ -Me–Al(C₆F₅)₂^{*i*}Bu (2b), which has a terminal isobutyl group on Al instead of a methyl group as in 2a. ¹H and ¹⁹F NMR spectra are presented in Figure S2.

When an excess of B(C₆F₅)₃ vs Al₂R₆ is used (ratio B:Al > 1, Scheme 2, bottom), aryl/alkyl group exchange occurs, but some pentafluorophenyl ligands remain bound to boron so that a mixture of B(C₆F₅)_{*x*}R_{3–*x*} and Al(C₆F₅)₃ is created. The subsequent reaction with Cp*₂ZrMe₂ results in a mixture of two methyl-bridged ion pairs, Cp*₂Zr(Me)– μ -Me–Al(C₆F₅)₃ (1) and Cp*₂Zr(Me)– μ -Me–B(C₆F₅)₃ (4), for which Figure 2 depicts the ¹H and ¹⁹F NMR spectra at 20 °C (reagent ratio B:Al:Zr = 2:1:1). All chemical shifts are listed in Table S1. Ion pair 1 was structurally characterized by single-crystal X-ray diffraction (Figure 3). Similar crystal structures have been reported for L₂Zr(Me)– μ -Me–Al(C₆F₅)₃ (L = 1,2-(CH₃)₂C₅H₃; (CH₃)₄-C₅H)^{26,27}. The structure of ion pair 1 differs from those reported earlier in that the bridging methyl group is significantly more “abstracted” by the aluminum moiety in 1, which may be attributed to the steric environment caused by the Cp* ligands (as reflected by the bite angle between the two Cp* planes of 41.4°).

b. Activation of Cp*₂ZrMe₂ with [Ph₃C][B(C₆F₅)₄] and Al₂R₆. Several experiments were conducted to study the reaction of [Ph₃C][B(C₆F₅)₄], Al₂R₆, and Cp*₂ZrMe₂. The mechanism of activation depends on whether Al₂Me₆ or Al₂^{*i*}Bu₆ is used in combination with [Ph₃C][B(C₆F₅)₄]. Rapid discoloration of the orange solution was observed when [Ph₃C][B(C₆F₅)₄] was mixed with Al₂^{*i*}Bu₆, which was attributed to the disappearance of the trityl cation. The reaction involves hydride abstraction and isobutene elimination to form transient cationic aluminum species [Al^{*i*}Bu₂]⁺, which reacts further by fast transfer of the

Scheme 3. The Reaction of [Ph₃C][B(C₆F₅)₄], Al₂Me₆ and Cp*₂ZrMe₂ Results in the Formation of Ion Pair 5 ([Cp*₂Zr–(μ -Me)₂–AlMe₂][B(C₆F₅)₄])

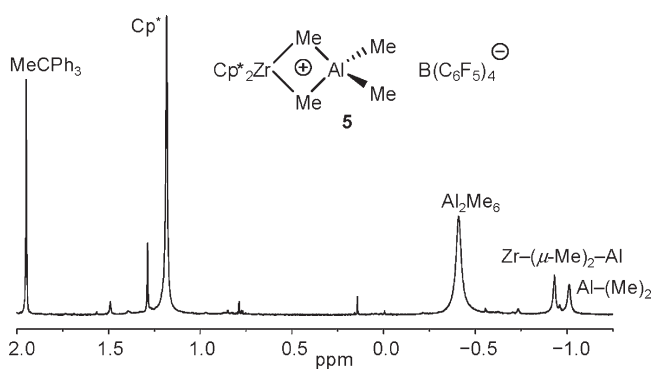
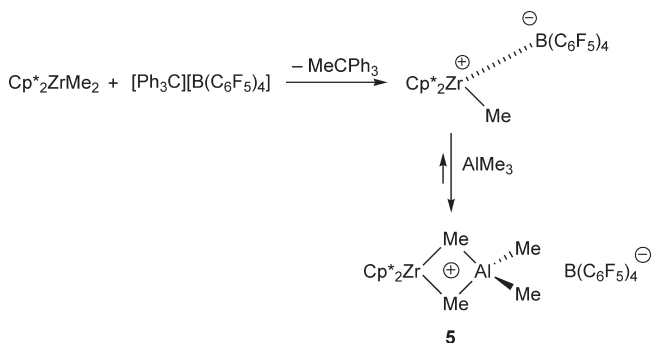


Figure 4. ¹H NMR spectrum in toluene-*d*₈ at 20 °C of the reaction of [Ph₃C][B(C₆F₅)₄], Al₂Me₆, and Cp*₂ZrMe₂ (ratio 1:2:1), resulting in the formation of ion pair 5.

C₆F₅ groups from boron to aluminum.¹⁶ The reaction affords the same methyl-bridged species as when B(C₆F₅)₃ and Al₂^{*i*}Bu₆ are used (Scheme S1). However, [Ph₃C][B(C₆F₅)₄] transfers four C₆F₅ groups, while B(C₆F₅)₃ transfers only three.

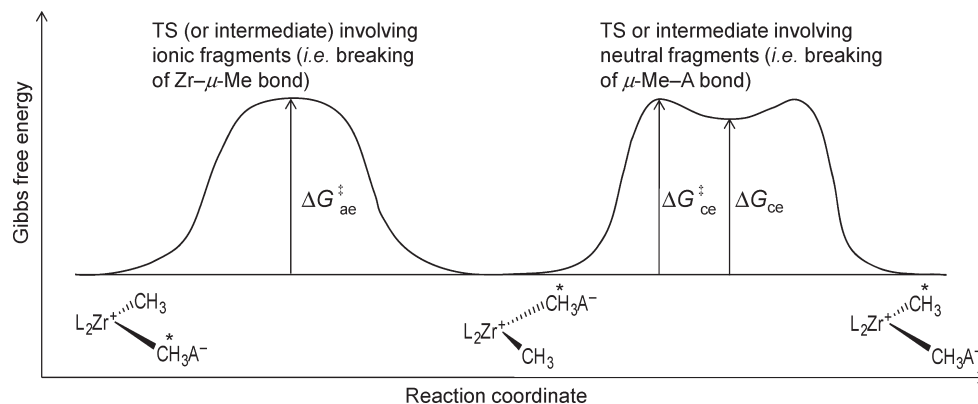
The trityl cation does not react with Al₂Me₆; that is, no discoloration of the solution was observed, indicating that no methide abstraction occurred that would form an [AlR₂]⁺ transient species. Therefore, the borate anion remains unaffected when [Ph₃C][B(C₆F₅)₄] is mixed with Al₂Me₆.¹⁶ Upon addition of Cp*₂ZrMe₂, the trityl cation abstracts a methide from Zr to form the complex [Cp*₂Zr–(μ -Me)₂–AlMe₂]⁺[B(C₆F₅)₄][–] (5) (Scheme 3). The ¹H NMR spectrum of ion pair 5 is shown in Figure 4. The cation [Cp*₂Zr–(μ -Me)₂–AlMe₂]⁺ is in equilibrium with the “free” zirconocenium cation [Cp*₂ZrMe]⁺. When the amount of Al₂Me₆ is increased, the equilibrium shifts toward ion pair 5, which thus decreases the activity of the catalyst (see below).^{3,17,31}

It is worth mentioning that bridged cations of the form [L₂Zr(Me)– μ -Me–(Me)ZrL₂]⁺ (L = Cp, Me₂Si(Ind)₂, C₂H₄-(Ind)₂) were reported by Bochmann,^{31,32} but that no similar species was observed under any conditions used in this study. This might be caused by the high steric demands of the Cp* ligands, preventing such dimer formation, as has also been suggested by Brintzinger and co-workers.¹²

Having identified the ion pairs that are generated under various conditions, as summarized in Table 2, we now turn to

Table 2. Summary of the Ion Pairs Generated by Reaction of Cp*₂ZrMe₂, a Boron-C₆F₅ Compound, and Al₂R₆

		Cp* ₂ ZrMe ₂			
		B(C ₆ F ₅) ₃		[Ph ₃ C][B(C ₆ F ₅) ₄]	
		Al ₂ Me ₆	Al ₂ ⁱ Bu ₆	Al ₂ ⁱ Bu ₆	Al ₂ Me ₆
B:Al < 1	Al ₂ R ₆ in soln.				
B:Al > 1					

Scheme 4. Schematic Reaction Coordinates for the Reorganization Processes of Zirconocenium Ion Pairs^a

^a Left: anionic exchange pathway (ae) via dissociation of the Zr- μ -Me bond. Right: cocatalyst exchange pathway (ce) via dissociation of the μ -Me-A bond.

study the dynamics of these solutions. The dynamics associated with ion pair **5** will be treated in another report.³³

II. Dynamic NMR Study of Solutions Containing Ion Pairs **1 and **2a**.** As previously described by Marks and co-workers,^{27,34} the anionic moiety of the ion pair can migrate between the two available sites on zirconium by two spectroscopically differentiable rearrangement processes. The first pathway, called anionic exchange (ae, Scheme 4, left), implies a transition state in which the transient [L₂ZrMe]⁺ species dissociates from the anionic Lewis base. Such a pathway does not lead to coalescence of NMR signals for catalysts with symmetrical ligands on zirconium (e.g., Cp*₂ZrMe₂). The second process, called cocatalyst exchange (ce, Scheme 4, right), leads to the migration of the activator A to the other site on Zr via dissociation of the μ -Me-A bond and hence implying fragmentation into neutral species.^{7,34} Such a pathway leads to the coalescence of the terminal and bridged methyl signals of the ion pair.

The NMR spectra of the mixture of ion pairs **1** and **2a** exhibit broadening of several methyl signals due to the structural rearrangement processes explained above and due to other methyl exchange reactions (see below). Two mixtures were subjected to dynamic NMR experiments: a mixture containing only the ion pairs **1** and **2a**, prepared by reaction of B(C₆F₅)₃, Al₂Me₆, and

Cp*₂ZrMe₂ in a 1:1:1 molecular ratio, and a mixture containing additionally a residual amount of Al₂(C₆F₅)_xMe_{6-x} ($x = 0, 1$), prepared from the same reagents in a 1:2:1 molecular ratio. Figures 5 and 6 display the experimental and simulated spectra for both solutions, and Figures 7 and 8 show the Eyring plots obtained from line shape analysis. Scheme 5 and points 1–3 describe the mechanisms that are proposed for the methyl group exchanges observed by NMR; all thermodynamic results are presented in Table 3.

1. Ion pair **2a**: The signals of methyl groups A and B of ion pair **2a** broaden and coalesce in the NMR spectra due to cocatalyst exchange (see above). The rate constant k_{AB} was used for determining the thermodynamic parameters for this exchange reaction (i.e., $k_{AB} = k_{ce}$), affording $\Delta_r G^\ddagger = 13.3(10)$ and $13.9(12)$ kcal mol⁻¹ at 298 K without and with a residual amount of Al₂(C₆F₅)_xMe_{6-x} ($x = 0, 1$), respectively. These Gibbs free energy barriers agree within their uncertainties.
2. Ion pair **1**: The ¹H NMR signal for the terminal Zr-Me group of **1** remains sharp until at least 80 °C (Figure 9, methyl Z), suggesting that a cocatalyst exchange reaction similar to that observed for **2a** does not occur for **1**. Such a

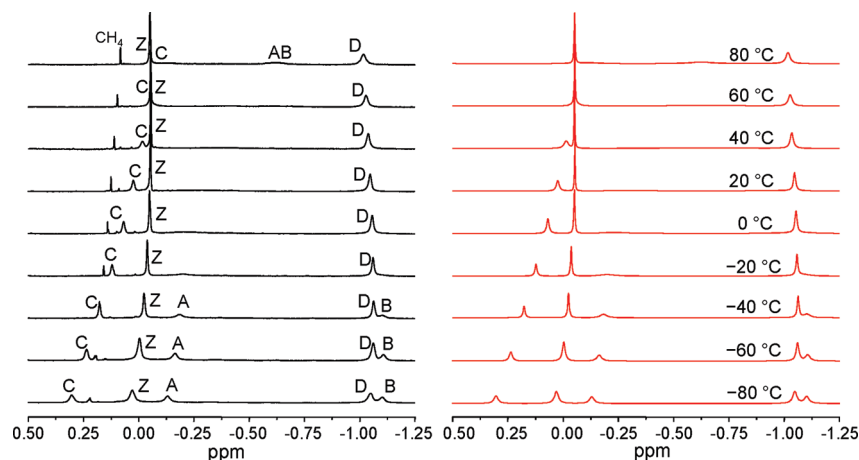


Figure 5. Experimental (left) and simulated (right) temperature-dependent ^1H NMR spectra of a mixture of ion pairs **1** and **2a**. Peak labels correspond to the assignments in Scheme 5.

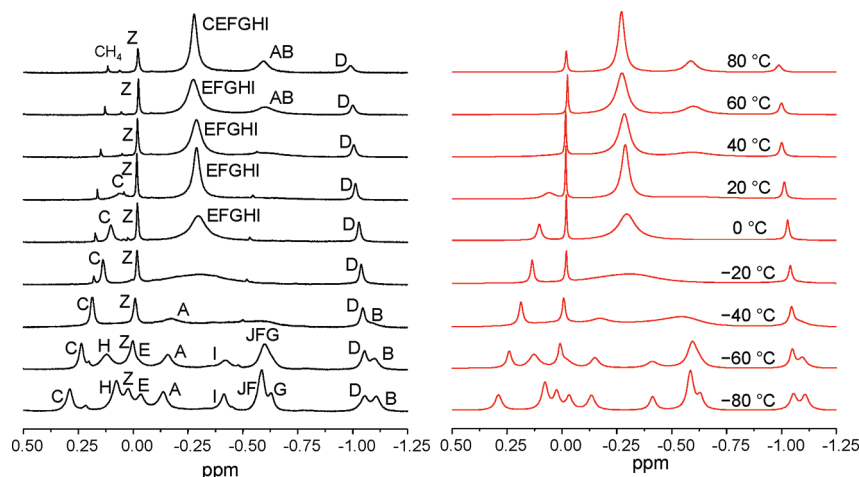
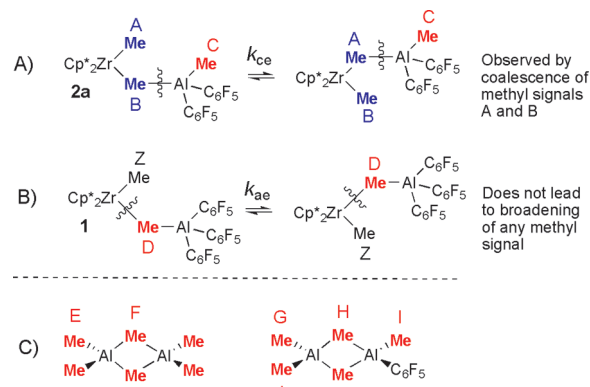


Figure 6. Experimental (left) and simulated (right) temperature-dependent ^1H NMR spectra of a mixture of species **1**, **2a**, and $\text{Al}_2(\text{C}_6\text{F}_5)_x\text{Me}_{6-x}$ ($x = 0, 1$).

“ce” process would lead to a broadening of both the bridging and terminal methyl signals of the ion pair. For **1**, only a broadening of the bridging methyl signal is observed (Figure 9, methyl D), which thus must arise from a pathway involving the dissociation of the $\text{Zr}-\mu\text{-Me}$ bond. Simultaneously, a broadening of the terminal methyl on Al in ion pair **2a** (methyl C) is observed. Therefore, we propose a mechanism in which these methyl groups exchange by the involvement of a transient species $\text{AlMe}(\text{C}_6\text{F}_5)_2$ of low concentration, which is unobservable in the NMR spectra (Scheme S2). In our simulations, we approximated this reaction by a direct exchange of methyl group C with D. Furthermore, as this reaction involves dissociation of the $\text{Zr}-\mu\text{-Me}$ bond of **1**, we conclude that an anionic exchange should also occur but cannot be observed due to the symmetry of **1**. In conclusion, for ion pair **1** cleavage of the $\mu\text{-Me}-\text{Al}$ bond requires considerably more energy than the breaking of the $\text{Zr}-\mu\text{-Me}$ bond.

3. $\text{Al}_2(\text{C}_6\text{F}_5)_x\text{Me}_{6-x}$ ($x = 0, 1$): At -80°C , the spectrum exhibits six nearly resolved methyl signals for $\text{Al}_2(\text{C}_6\text{F}_5)_x\text{Me}_{6-x}$ ($x = 0, 1$), which coalesce to a single chemical shift at higher temperatures. For the simulations we presumed that the

Scheme 5. Methyl Group Exchange Reactions for a Solution Containing Ion Pairs **1 and **2a** (A and B) and for a Solution Containing Ion Pairs **1**, **2a**, and $\text{Al}_2(\text{C}_6\text{F}_5)_x\text{Me}_{6-x}$ (A–C)**



exchange reactions occurring for the methyl groups of Al_2Me_6 and $\text{Al}_2(\text{C}_6\text{F}_5)\text{Me}_5$ follow similar kinetics. They were therefore approximated with a single rate constant

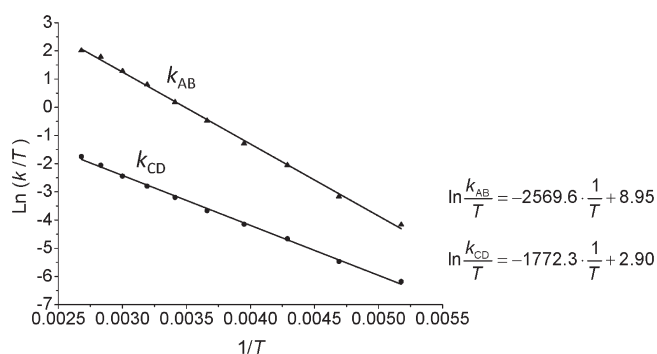


Figure 7. Eyring plots for the cocatalyst exchange reaction of **2a** (triangles) and for the methyl exchange CD (circles) for the solution without residual $\text{Al}_2(\text{C}_6\text{F}_5)_x\text{Me}_{6-x}$ ($x = 0, 1$).

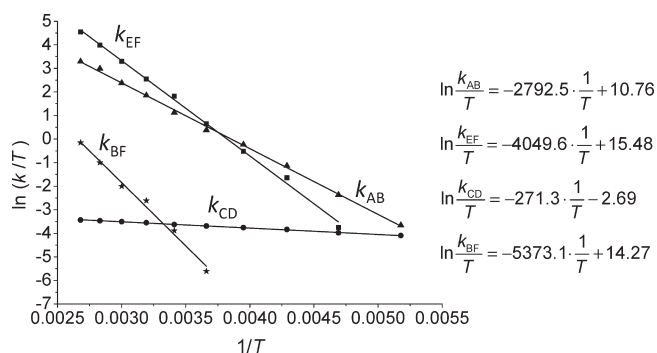


Figure 8. Eyring plots for the cocatalyst exchange reaction of **2a** (triangles), the methyl exchange CD (circles), the methyl exchange CE (stars), and the methyl exchange for $\text{Al}_2(\text{C}_6\text{F}_5)_x\text{Me}_{6-x}$ ($x = 0, 1$) (squares).

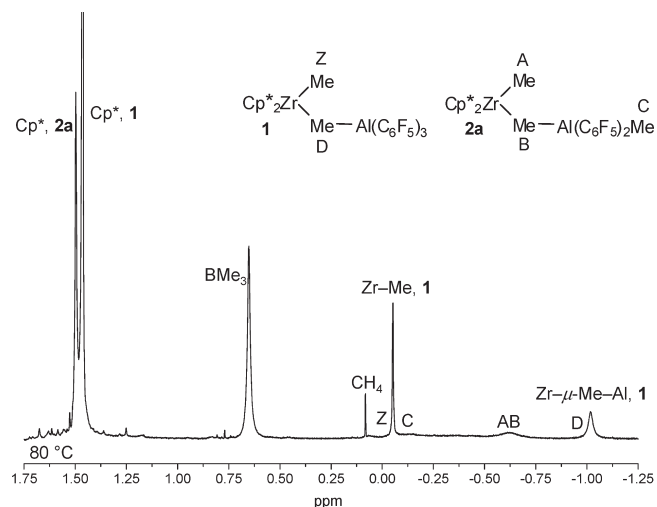


Figure 9. ^1H NMR spectrum at 80°C of ion pairs **1** and **2a**. A sharp signal for the terminal $\text{Zr}-\text{Me}$ group of **1** is observed at -0.05 ppm.

k_{EF} . We also observed an exchange reaction occurring between the methyl groups of $\text{Al}_2(\text{C}_6\text{F}_5)_x\text{Me}_{6-x}$ ($x = 0, 1$) and the methyl resonance **C** of **2a**, which we simulated with a fourth rate constant, k_{CE} . This reaction probably also involves the transient $\text{AlMe}(\text{C}_6\text{F}_5)_2$ species postulated for the exchange of methyl resonance **C** with **D** of **1** (see point 2). For the

exchange of the $\text{Al}_2(\text{C}_6\text{F}_5)_x\text{Me}_{6-x}$ ($x = 0, 1$) methyl groups, we obtained a $\Delta_r G^\ddagger = 13(2)$ kcal mol $^{-1}$ at 298 K.

DNMR Discussion. Table 3 summarizes our experimental data and includes literature values for cocatalyst exchange and anionic exchange of systems closely analogous to ours. For the ion pair *rac*-(EBI)Zr(Me)- μ -Me-Al(C_6F_5) $_3$ (EBI = $\text{C}_2\text{H}_4(\text{Ind})_2$), Marks and co-workers²⁷ reported $\Delta_r G_{\text{ae}}^\ddagger(298\text{ K}) \approx 21$ and $\Delta_r G_{\text{ce}}^\ddagger(298\text{ K}) \approx 20$ kcal mol $^{-1}$ for “ae” and “ce” processes, respectively. That we find a lower energy barrier for the cocatalyst exchange process of **2a** is consistent with the fact that $\text{Al}(\text{C}_6\text{F}_5)_2\text{Me}$ is a weaker Lewis acid than $\text{Al}(\text{C}_6\text{F}_5)_3$. The negative entropy obtained for the “ce” of **2a** suggests that this reaction occurs via an associative pathway. We propose a transition state where an incoming $\text{Al}(\text{C}_6\text{F}_5)_2\text{Me}$ binds to the vacant methyl on zirconium to form a doubly activated ion pair. We already suggested above that $\text{Al}(\text{C}_6\text{F}_5)_2\text{Me}$ is present in solution at low concentration. Doubly activated ion pairs have been reported for several metallocenes activated with $\text{Al}(\text{C}_6\text{F}_5)_3$,²⁸ and also spectroscopic evidence has been reported for the formation of doubly $\text{B}(\text{C}_6\text{F}_5)_3$ -activated metallocene complexes as intermediates in intermolecular borane exchange processes.^{29,30}

Our DNMR data suggest that the anionic exchange process of **1** involves a lower barrier than a cocatalyst exchange process. This means that the “ae” process for **1** is probably more facile for our system than that reported by Marks for *rac*-(EBI)Zr(Me)- μ -Me-Al(C_6F_5) $_3$, as might be expected from the differences in the respective crystal structures (see above). This can be attributed to the steric congestion of the Cp^* ligands that weakens the cation/anion attraction and lowers the energy barrier for the dissociation into ionic fragments.⁸ In addition, ionic fragmentation will cause the largest relief of steric congestion at the zirconium center.

The value for the overall methyl exchange processes of $\text{Al}_2(\text{C}_6\text{F}_5)_x\text{Me}_{6-x}$ ($x = 0, 1$) is slightly higher than that reported in the literature for methyl exchange in Al_2Me_6 .³⁵ Yamamoto et al. determined $\Delta_r G^\ddagger(298\text{ K}) = 10.7(2)$ kcal mol $^{-1}$ in cyclopentane and claimed similar thermodynamics in toluene. This result is reasonable since we use a single rate constant for simulating the exchange reaction of both Al_2Me_6 and $\text{Al}_2(\text{C}_6\text{F}_5)\text{Me}_5$. The electron-withdrawing pentafluorophenyl group on Al should stabilize the dimeric form of $\text{Al}_2(\text{C}_6\text{F}_5)\text{Me}_5$, resulting in a higher energy barrier for methyl exchange. Furthermore, we obtained a negative entropy of activation, which suggests that the reaction proceeds in an associative manner under our conditions. In the literature, both inter- and intramolecular processes for methyl group exchange in Al_2Me_6 have been reported. A detailed analysis will be presented in future work.³³

III. DFT Calculations. We performed DFT calculations of the various zirconocenium ion pairs observed in the NMR study to compare their geometrical parameters. Two additional ion pairs, **3a** and **3b**, were taken into consideration that were not observed in the NMR study, having the chemical formula $\text{Cp}^*_2\text{Zr}(\text{Me})-\mu\text{-Me}-\text{Al}(\text{C}_6\text{F}_5)\text{Me}_2$ and $\text{Cp}^*_2\text{Zr}(\text{Me})-\mu\text{-Me}-\text{Al}(\text{C}_6\text{F}_5)^i\text{Bu}_2$, respectively. $\text{Al}(\text{C}_6\text{F}_5)\text{R}_2$ ($\text{R} = \text{Me}, ^i\text{Bu}$) is probably not Lewis acidic enough to form detectable ion pairs **3**. Nevertheless, the comparison of geometrical parameters along the series of ion pairs **1**–**2**–**3** is interesting to make from a theoretical point of view.

The geometries of ion pairs **1**, **2a**, **2b**, **3a**, **3b**, and **4** were optimized at the M06-L²⁴ level with the SDD basis set and pseudopotentials on all atoms, and the geometries are displayed in Figure S3. The overall geometry of ion pair **1** is in good agreement with the obtained crystal structure (Table S3), which

Table 3. Thermodynamic Data (in kcal mol⁻¹, $\Delta_r G^\ddagger$ at 298 K, $\Delta_r S^\ddagger$ in cal mol⁻¹ K⁻¹) for the DNMR Experiments in Toluene^a

species	ref	rate constant	pathway ^b	$\Delta_r G^\ddagger$	$\Delta_r H^\ddagger$	$\Delta_r S^\ddagger$
2a ^c		k_{AB}	ce	13.9(12)	5.1(8)	-29(3)
2a ^d		k_{AB}	ce	13.3(10)	5.6(8)	-26(3)
Al ₂ (C ₆ F ₅) _x Me _{6-x} (x = 0, 1) ^d		k_{EF}		13(2)	8.1(14)	-16(5)
exchange reaction of C (2a) with D (1) ^c		k_{CD}		15.9(8)	3.5(6)	-42(4)
exchange reaction of C (2a) with D (1) ^d		k_{CD}		16.2(10)	0.5(5)	-53(3)
<i>rac</i> -(EBI)Zr(Me)- μ -Me-Al(C ₆ F ₅) ₃	27		ae	≈21	≈16	≈-15
	27		ce	≈20	≈22	≈8
<i>rac</i> -(EBI)Zr(Me)- μ -Me-B(C ₆ F ₅) ₃	27		ae	18.5	14(2)	-15(2)
	27		ce	19.6	22(1)	8(2)
	36		ce	18.4		
(Me ₂ C ₅ H ₃) ₂ Zr(Me)- μ -Me-B(C ₆ F ₅) ₃	8		ae	18.3 ^e		
	8		ce	19.7 ^e		
((SiMe ₃) ₂)C ₅ H ₃) ₂ Zr(Me)- μ -Me-B(C ₆ F ₅) ₃	8		ae	14.4 ^f		
	8		ce	18.0 ^f		
Cp* ₂ Zr(Me)- μ -Me-B(C ₆ F ₅) ₃ (4)	8		ce	19.8 ^e		
Al ₂ Me ₆ ^g	35			10.7(2)	15.5(15)	15.9

^a Literature values are presented in the second part of the table. ^b ae and ce stand for anion exchange and cocatalyst exchange, respectively. ^c Mixture of ion pairs 1 and 2a. ^d Mixture of ion pairs 1, 2a, and residual Al₂(C₆F₅)_xMe_{6-x}. ^e At 80 °C. ^f At 35 °C. ^g In cyclopentane.

Table 4. Comparison of Selected Geometrical Parameters for the Calculated Structures (M06-L/SDD) of Ion Pairs 1, 2a, 2b, 3a, 3b, and 4 (distances [Å] and angles [deg]; 1–3, E = Al; 4, E = B)

	1	2a	2b	3a	3b	4
Zr–Me	2.259	2.265	2.257	2.257	2.261	2.251
Zr– μ -Me	2.530	2.477	2.505	2.457	2.470	2.605
μ -Me–E	2.031	2.072	2.065	2.122	2.115	1.673
distance Zr···E	4.547	4.542	4.567	4.579	4.552	4.275
μ -Me–Zr–Me	92.37	90.01	93.19	95.17	93.51	91.92
Zr– μ -Me–E	171.01	173.22	178.04	178.44	173.69	176.37

therefore supports the utilization of the calculated geometrical parameters for our discussion.

Three different approaches are used to draw conclusions from the geometries of the various ion pairs. First, we evaluate the role of the main-group atom E by comparing ion pairs 1 and 4. Next, we describe the influence of the number of pentafluorophenyl groups on Al, i.e., moving in the series from ion pair 1 to 3. Finally, we look at the influence of the type of alkyl groups (Me or ^tBu) by comparing ion pair 2a with 2b and 3a with 3b.

- Marks et al.²⁷ have reported that B(C₆F₅)₃ has significantly higher Lewis acidity and methide affinity than does Al(C₆F₅)₃. Our results are consistent with their findings, as the bond between zirconium and the bridging methyl group is longer in ion pair 4 than in ion pair 1 (Zr– μ -Me: 2.605 Å (4) vs 2.530 Å (1)).
- Along the series of ion pairs 1, 2, and 3, the Zr– μ -Me bond length decreases and the μ -Me–Al bond length increases, reflecting the decrease in Lewis acidity of the Al(C₆F₅)_n-R_{3-n} moiety with increasing n.
- The terminal alkyl groups on Al affect the geometry of the ion pair. The largest effect is observed for the Zr– μ -Me bond length with values of 2.530, 2.505, and 2.477 Å for 1, 2b, and 2a, respectively. The bond length for 2b is closer to that for 1

than 2a, which is probably due to the increased steric demands of the ^tBu group causing congestion with the Cp* ligands. This will also facilitate the formation of ionic fragments, which is important for the activity of the catalyst.

Having studied the geometries of the various ion pairs, we now investigate the activities in ethylene polymerization of the different catalytic solutions containing those ion pairs.

IV. Activity in Ethylene Polymerization. In this section we investigate the catalytic activities of solutions containing the various ion pairs described above. First we compare the catalytic systems with B(C₆F₅)₃ as the activator, which results in the formation of ion pairs 1, 2, and 4. Then, the activities of catalytic solutions containing ion pair 5 are discussed (see Schemes 2 and 3 for the chemical structures of the ion pairs).

From our NMR study it is possible to predict which ion pairs are present in solution for given initial reactant ratios. In order to investigate the activities of the various ion pairs in ethylene polymerization, a series of polymerization experiments was conducted in which the type and ratios of the reagents were modified. Two main differences in the conditions used for the NMR study and the polymerization experiments may influence the formation and ratios of the ion pairs present in the catalytic mixture: (1) the concentrations used for the NMR experiments were higher than for the polymerization experiments ($c_{\text{cat}} = 25$ vs 1 mM) and (2) a minimum of 5 equivalents of Al₂R₆ relative to Zr was used to increase the reproducibility of the polymerization results.

For our polymerization experiments, we applied a preactivation period of 3 min, during which all reactants were mixed under an argon atmosphere before the introduction of ethylene. Thus, formation of the ion pairs studied by NMR spectroscopy was ensured, and an induction period arising from slow formation of the active species was prevented. Otherwise, different ion pairs may form that may also be active in ethylene polymerization, especially when the conditions prevent transfer of C₆F₅ groups, such as when ethylene is added before B(C₆F₅)₃ and Cp*₂ZrMe₂.

Table 5. Data of Ethylene Polymerization Catalyzed by $B(C_6F_5)_3$, Al_2R_6 ($R = Me, ^iBu$), and $Cp^*_2ZrMe_2$ ($c = 1 \times 10^{-3} M$) at 40 °C and 2 bar (1 bar ethylene +1 bar Ar) for 3 min

entry	R	ratio (B:Al:Zr)	ion pair present ^a	activity ^b	M_n [Da]	PDI	N_{chains}/N_{Zr}
1	Me	10:5:1	4, 1	79	5405	1.79	0.41
2	ⁱ Bu	10:5:1	4, 1	66	4913	1.58	0.43
3	Me	5:5:1	1	75	7431	1.52	0.33
4	ⁱ Bu	5:5:1	1	97	6234	1.71	0.46
5	Me	2.5:5:1	1, 2a	83	9262	2.11	0.21
6	ⁱ Bu	2.5:5:1	1, 2b	100	10060	1.71	0.29
7	Me	1:5:1	2a, (1)	1			
8	ⁱ Bu	1:5:1	2b, (1)	65	11 861	1.61	0.17
9	Me	1:20:1	2a	10	2534	1.47	0.14
10	ⁱ Bu	1:20:1	2b	77	7196	2.29	0.23

^a From NMR study. ^b [kgPE mol Zr⁻¹ h⁻¹ bar⁻¹].

We note that the correlation between the observed species in NMR and the activity observed in ethylene polymerization is delicate because the most abundant species in solution may not be the major contributor to activity. Furthermore, mass transport limitation is a common drawback for precise determination of catalytic activities, especially for ethylene polymerization.³ Nevertheless, we could correlate the activity in ethylene polymerization of the different reaction mixtures with the presence of the ion pairs identified by NMR.

Table 5 lists the results of the polymerization experiments catalyzed by mixtures of $B(C_6F_5)_3$, Al_2R_6 , and $Cp^*_2ZrMe_2$ at different reagent ratios. The table gives the predicted ion pairs present in solution (based on the NMR study), the polymerization activities, and the polymer molecular structure. The following observations can be made:

1. The catalytic mixtures containing ion pairs **1** and **4** were both active in ethylene polymerization and afforded similar activities and polymer molecular structures (Table 5, entries 1–4). The comparable results for entries 1 vs 2 and 3 vs 4 are in agreement with the fact that the formation of ion pairs **1** and **4** is independent of the alkylaluminum species used.
2. The catalytic solutions containing ion pair **2a** showed very low activity, whereas those containing ion pair **2b** were comparable in activity to solutions of ion pairs **1** and **4** (Table 5, entries 7–10). Therefore, the replacement of the methyl group on Al by isobutyl in ion pair **2** is sufficient to improve catalyst activity. This suggests easier ionic dissociation of ion pair **2b** as compared to **2a**, which is in agreement with the calculated longer Zr– μ -Me and shorter μ -Me–Al bonds.
3. The number of polymer chains produced relative to the available Zr centers (N_{chains}/N_{Zr}) was notably lower for the catalytic solutions containing ion pair **2b** (and also **2a**) than for those containing ion pairs **1** and **4** (Table 5). This can be explained by a lower proportion of active centers generated by dissociation of ion pair **2b** (and **2a**), which is a result of the lower Lewis acidity of Al– $(C_6F_5)_2^iBu$ as compared to Al– $(C_6F_5)_3$ in **1**. The difference in polymerization activities was not as pronounced as that in the number of polymer chains, probably because of mass-transport limitation.

The reaction of $[Ph_3C][B(C_6F_5)_4]$, Al_2Me_6 , and $Cp^*_2ZrMe_2$ leads to the formation of the contact ion pair **5**, which is in

equilibrium with the loose ion pair $Cp^*_2ZrMe^+ \cdots [B(C_6F_5)_4]^-$ (Scheme 3). As previously described,³ we observed that increasing the amount of Al_2Me_6 decreases the activity of ion pair **5** (Figure S4). Conversely, increasing the amount of $[Ph_3C][B(C_6F_5)_4]$ slightly improved the catalytic activity (Figure S4). This has been explained by Bochmann with the “trityl effect”,^{38,39} according to which the increase in activity is due to the aggregation of the metallocenium ion pair with $[Ph_3C][B(C_6F_5)_4]$.

CONCLUSION

In this work, we describe the activation mechanism of a zirconocene precatalyst with classical reagent combinations, i.e., with different combinations of a boron pentafluorophenyl compound and an aluminum alkyl species. Using NMR techniques, we show that different ratios of various ion pairs are formed depending on the activators and their respective ratios.

Most of the reagent combinations studied in this work lead to a mixture of ion pairs **1**, **2a/2b**, and **4** (Table 2), which is the result of transmetalation of pentafluorophenyl groups between the activators, i.e., from boron to aluminum. Therefore, the ratio of the formed ion pairs is highly dependent on the initial ratio of the activators. The catalytic solutions containing ion pairs **1**, **2b**, and **4** all actively catalyze the polymerization of ethylene. Polymerization data indicate that the solutions containing the ion pair **2a** were inactive. Accordingly, DFT calculations suggest a tighter ion pair for **2a** than for **2b**. When the transmetalation of the pentafluorophenyl groups is suppressed, ion pair **5** forms irrespective of the initial activator ratio. The activity of this catalyst system is still influenced by the amount of Al_2Me_6 .

Using DNMR techniques, we investigated the dynamics of two solutions containing ion pairs **1** and **2a** in the presence and absence of $Al_2(C_6F_5)_xMe_{6-x}$ ($x = 0, 1$). For the cocatalyst exchange process of **2a**, we obtained $\Delta_r G^\ddagger = 13.6(12)$ kcal mol⁻¹ at 298 K. Concerning ion pair **1**, the energy barrier for cocatalyst exchange, involving breaking of the μ -Me–Al bond, lies well above that for anionic exchange, involving breaking of the Zr– μ -Me bond. Furthermore, the shapes of the dynamic NMR spectra reveal that most methyl groups are labile, which reflects the difficulty of defining the composition of solutions and the nature of active species when performing a polymerization experiment.

To conclude, we show in this work that the transfer of pentafluorophenyl groups from boron to aluminum, often referred to as a deactivation pathway,¹⁶ may be the origin of the formation of active catalytic mixtures.

ASSOCIATED CONTENT

S Supporting Information. Additional NMR spectra and reaction schemes, calculated structures of the various ion pairs, and polymerization activities of ion pair **5**. This material is available free of charge via the Internet at <http://pubs.acs.org>.

AUTHOR INFORMATION

Corresponding Author

*E-mail: chen@org.chem.ethz.ch.

ACKNOWLEDGMENT

The authors acknowledge the support from the ETH Zürich and the Swiss National Science Foundation. We gratefully

acknowledge Dr. Andreas Bach for fruitful discussions, especially concerning DFT calculations.

REFERENCES

- (1) Bochmann, M. *Organometallics* **2010**, *29*, 4711–4740.
- (2) Chen, Y.-X.; Marks, T. J. *Chem. Rev.* **2000**, *100*, 1391–1434.
- (3) Bochmann, M. *J. Organomet. Chem.* **2004**, *689*, 3982–3998.
- (4) Macchioni, A. *Chem. Rev.* **2005**, *105*, 2039–2073.
- (5) Fujita, T.; Makio, H. In *Comprehensive Organometallic Chemistry III*, Vol. 11; Elsevier, 2007; pp 692–697, and references therein.
- (6) Janiak, C.; Versteeg, U.; Lange, K. C. H.; Weimann, R.; Hahn, E. *J. Organomet. Chem.* **1995**, *501*, 219–234.
- (7) Luo, L.; Marks, T. J. *Top. Catal.* **1999**, *7*, 97–106.
- (8) Yang, X.; Stern, C.; Marks, T. J. *J. Am. Chem. Soc.* **1994**, *116*, 10015–10031.
- (9) Ystenes, M.; Eilertsen, J. L.; Liu, J.; Ott, M.; Rytter, E.; Stovngeng, J. A. *J. Polym. Sci., Part A: Polym. Chem.* **2000**, *38*, 3450–3450.
- (10) Henderson, L. D.; Piers, W. E. *J. Organomet. Chem.* **2007**, *692*, 4661–4668.
- (11) Tritto, I.; Donetti, R.; Sacchi, M. C.; Locatelli, P.; Zannoni, G. *Macromolecules* **1997**, *30*, 1247–1252.
- (12) Beck, S.; Prosenč, M.-H.; Brintzinger, H.-H.; Goretzki, R.; Herfert, N.; Fink, G. *J. Mol. Catal. A* **1996**, *111*, 67–79.
- (13) Beringhelli, T.; Donghi, D.; Maggioni, D.; D'Alfonso, G. *Coord. Chem. Rev.* **2008**, *252*, 2292–2313.
- (14) Brintzinger, H. H.; Fischer, D.; Müllhaupt, R.; Rieger, B.; Waymouth, R. M. *Angew. Chem., Int. Ed. Engl.* **1995**, *34*, 1143–1170.
- (15) In solution, the dimeric species Al_2R_6 are in equilibrium with their monomeric form, the exact equilibrium constant depending on R and on temperature. For consistency and clarity of the data presentation, we always use the notation Al_2R_6 (R = Me, ⁱBu), even though Al_2^iBu_6 is essentially unassociated (monomeric) in solution.
- (16) Bochmann, M.; Sarsfield, M. J. *Organometallics* **1998**, *17*, 5908–5912.
- (17) Bochmann, M.; Lancaster, S. J. *J. Organomet. Chem.* **1995**, *497*, 55–59.
- (18) Klosin, J.; Roof, G. R.; Chen, E. Y.-X.; Abboud, K. A. *Organometallics* **2000**, *19*, 4684–4686.
- (19) M06-L/SDD calculations provided homolytic bond strengths of 105.9 (Me–BMe₂), 126.1 (C₆F₅–BMe₂), 86.9 (Me–AlMe₂), and 109.8 kcal mol⁻¹ (C₆F₅–AlMe₂). Hence, the transfer of a C₆F₅ moiety from boron to aluminum in exchange for a methyl group is net exothermic by about 2.7 kcal mol⁻¹. In accordance, the reaction $\text{B}(\text{C}_6\text{F}_5)_3 + \text{AlMe}_3 \rightarrow \text{BMe}_3 + \text{Al}(\text{C}_6\text{F}_5)_3$ was calculated to be 7.7 kcal mol⁻¹ exothermic, which outweighs the energy required to break up 1/2 equiv of dimeric Al_2Me_6 (6.6 kcal mol⁻¹).
- (20) At least to some extent, the aryl/alkyl group exchange was also observed when Al_2Me_6 was added to the preformed zirconocenium/borate. However, the quality of the resulting NMR spectrum was low, which was probably due to the high reactivity and sensitivity of the zirconocenium/borate ion pair when it is present in solution without alkyl aluminum species.
- (21) Janiak, C.; Lassahn, P.-G. *Macromol. Symp.* **2006**, *236*, 54–62.
- (22) Piers, W. E. *Adv. Organomet. Chem.* **2005**, *52*, 49–51.
- (23) (a) Manriquez, J. M.; McAlister, D. R.; Sanner, R. D.; Bercaw, J. E. *J. Am. Chem. Soc.* **1978**, *100*, 2716–2724. (b) Miller, F. D.; Sanner, R. D. *Organometallics* **1988**, *7*, 818–825.
- (24) Zhao, Y.; Truhlar, D. G. *Acc. Chem. Res.* **2008**, *41*, 157–167.
- (25) iNMR: <http://www.inmr.net>.
- (26) Liu, Z.; Somsook, E.; Landis, C. R. *J. Am. Chem. Soc.* **2001**, *123*, 2315–2316.
- (27) Stahl, N. G.; Salata, M. R.; Marks, T. J. *J. Am. Chem. Soc.* **2005**, *127*, 10898–10909.
- (28) Chen, Y.-X.; Kruper, W. J.; Roof, G.; Wilson, D. R. *J. Am. Chem. Soc.* **2001**, *123*, 745–746.
- (29) Al-Humydi, A.; Garrison, J. C.; Youngs, W. J.; Collins, S. *Organometallics* **2005**, *24*, 193–196.
- (30) Green, M. L. H.; Sassmannshausen, J. *Chem. Commun.* **1999**, 115–116.
- (31) Bochmann, M.; Lancaster, S. J. *Angew. Chem., Int. Ed. Engl.* **1994**, *33*, 1634–1637.
- (32) Lancaster, S. J.; Bochmann, M. *J. Organomet. Chem.* **2002**, *654*, 221–223.
- (33) Manuscript in preparation.
- (34) Deck, P. A.; Beswick, C. L.; Marks, T. J. *J. Am. Chem. Soc.* **1998**, *120*, 1772–1784.
- (35) Yamamoto, O.; Hayamizu, K.; Yanagisawa, M. *J. Organomet. Chem.* **1974**, *73*, 17–25, and references therein.
- (36) Siedle, A. R.; Newmarks, R. A. *J. Organomet. Chem.* **1995**, *497*, 119–125.
- (37) Liu, Z.; Somsook, E.; White, C. B.; Rosaaen, K. A.; Landis, C. R. *J. Am. Chem. Soc.* **2001**, *123*, 11193–11207.
- (38) Song, F.; Cannon, R. D.; Lancaster, S. J.; Bochmann, M. *J. Mol. Catal. A* **2004**, *218*, 21–28.
- (39) Alonso-Moreno, C.; Lancaster, S. J.; Zuccaccia, C.; Macchioni, A.; Bochmann, M. *J. Am. Chem. Soc.* **2007**, *129*, 9282–9283.